Applied Catalysis B: Environmental 132–133 (2013) 107–115

Contents lists available at SciVerse ScienceDirect

Applied Catalysis B: Environmental

journal homepage: www.elsevier.com/locate/apcatb

Gold nanoparticle decorated ceria nanotubes with significantly high catalytic activity for the reduction of nitrophenol and mechanism study

Jianming Zhang, Guozhu Chen*, Mohamed Chaker, Federico Rosei, Dongling Ma*

Institut National de la Recherche Scientifique, INRS-Énergie, Matériaux et Télécommunications, 1650 Boulevard Lionel-Boulet, Varennes, Québec J3X 1S2, Canada

ARTICLE INFO

Article history:
Received 3 August 2012
Received in revised form 9 November 2012
Accepted 21 November 2012
Available online 29 November 2012

Keywords:
Au nanoparticle
CeO_2
Hydrogenation
Nitrophenol reduction
Laser ablation

ABSTRACT

We report the preparation and catalytic properties of a new nanostructured catalyst, made of small (~5 nm in diameter) and uniform gold nanoparticles (AuNPs) and ceria nanotubes (CeO_2 NTs). "Surfactant-free" AuNPs fabricated by pulsed laser ablation in liquid (PLAL) on a bulk Au target are efficiently assembled onto the surface of CeO_2 NTs without performing any surface functionalization of either component to promote their coupling, thanks to the presence of —OH on the PLAL-AuNPs. The reduction reaction of 4-nitrophenol into 4-aminophenol catalyzed by our PLAL-AuNP/CeO_2-NT catalyst exhibits remarkably higher reaction rate in comparison to that catalyzed by similar catalysts composed of chemically prepared AuNPs (Chem-AuNPs) as an active phase and/or commercially available CeO_2 powder as support. Their superior catalytic activity is found to be due to the unique, relatively "bare" surface of the PLAL-AuNPs as well as oxidized Au species induced by the strong interaction between the "barrier-free" surface of PLAL-AuNPs and surface defects (oxygen vacancies) of CeO_2 NTs. The important role of unique surface chemistry of PLAL-AuNPs in catalysis was further demonstrated in CO oxidation reaction in gas phase. Our results suggest that the use of PLAL-AuNPs enables easy and efficient attachment of AuNPs onto the surface of the CeO_2 NTs and their unique combination leads to the development of highly efficient catalysts. Our design and fabrication of the nanocatalysts take full advantage of the unique features of the PLAL-AuNPs and potentially constitute a general and efficient route to prepare other metal-NP/metal-oxide-support catalysts, which can therefore largely expand the applications of PLAL-noble metal NPs in catalysis.

1. Introduction

Since the seminal work of Haruta [1], AuNPs have attracted considerable attention because they show specific catalytic properties, which the bulk material does not possess, and hold great potential in many applications, such as selective hydrogenation of nitro-aromatic compounds, carbon monoxide (CO) oxidation, and water–gas shift reaction [2–28]. Nitro-aromatic compounds as toxic organic by-products are generally produced undesirably during the industrial manufacturing process of chemicals, such as agrochemicals, dyes and pharmaceuticals [29,30]. In the presence of AuNP based catalyst, the nitro-aromatic compounds can be efficiently reduced into their corresponding useful aromatic amines [41–49]. Although in principle, smaller NPs show higher catalytic activity, they easily aggregate due to their high surface energy, resulting in a large reduction of their catalytic activity [2,5]. To overcome this problem, appropriate stabilizers, such as surfactants and functional molecules, are required to control NP nucleation/growth, prevent coalescence and/or link NPs to support materials during wet chemical synthesis [2,5,11–18,27,28]. Nevertheless, it is also noted that the presence of these molecules on NP surface can obstruct the access of reactants to the active sites of NPs and thus decrease their catalytic activity [5]. To remove these stabilizing molecules, extensive washing or extra thermal treatment to NPs has to be conducted. In most cases, unfortunately, these treatments cause a size increase and even agglomeration, which degrade the final catalytic activity of these NPs [5,14,15]. It has been reported that impregnation-incipient wetness, deposition–precipitation (DP) and in situ growth on support materials are other well established approaches to synthesize small AuNPs without using stabilizing molecules [2,10,11,14,15,19–23,44]. Nonetheless, impurities, such as chloride ion (Cl^-) from $HAuCl_4$ precursor or sodium carbonate from DP method, remaining in the catalyst must be completely removed by exhaustive washing treatment since these substances exert negative impact on Au catalysts [2]. In particular, the Cl^- residue not only poisons Au catalysts but also favors NP aggregation at high temperature by promoting mobilization of Au atoms [19–21]. On the other hand, pulse laser ablation on a Au bulk target in gas or liquid phase as an increasingly important "top down" method provides an

* Corresponding authors. Tel.: +1 514 228 6920; fax: +1 450 929 8102.
E-mail addresses: chen@emt.inrs.ca (G. Chen), ma@emt.inrs.ca (D. Ma).

0926-3373/$ – see front matter © 2012 Elsevier B.V. All rights reserved.
http://dx.doi.org/10.1016/j.apcatb.2012.11.030

alternative way to produce relatively "bare and clean" AuNPs [31–39], which are expected to favor catalytic reactions because the reactive sites on the NP surface are mostly exposed and readily accessible for reactants during catalytic reactions. Accordingly, AuNPs prepared by laser ablation technique are anticipated to act as highly promising catalysts.

As far as the laser technique for preparing NPs is concerned, supported AuNP catalysts have successfully been prepared by pulsed laser deposition (PLD) on substrates (such as Fe_2O_3, SiO_2 and MnO_2) in a close chamber filled with certain gas [37–39]. And these supported AuNPs exhibit high catalytic efficiency in various gas phase catalytic reactions of oxidizing small organic molecules [37–39]. Although the use of stabilizing chemicals is avoided in this PLD approach, which prevents the contamination of metal NPs, the set-up and operation of PLD system are rather complicated in practice as well as time-consuming. In contrast, pulsed laser ablation in liquid phase (PLAL) offers significant convenience in experimental manipulation. In addition, if appropriately optimized, it is able to yield small, mono-disperse, stable colloidal NPs without intentionally introducing any stabilizing molecules. In particular, this technique can endow unique surface-chemistry features to the AuNPs, due to the high density and temperature of the laser plasma plume in liquid [36], but not available from other synthetic approaches. For example, Luong et al. and our group reported that Au atoms on the surface of freshly prepared AuNPs by laser technique in water are partially oxidized [31,34], Kondow [32], Muniz-Miranda et al. [33] and our group [35] also showed that small OH^- groups from aqueous environment adsorb on the PLAL-metal NP surface to form a negatively charged surface to stabilize the NPs. These small OH^- groups are expected to impose much less "barrier" effects on catalysis than most stabilizing molecules, which are generally much larger and can block the access of reactant molecules to the catalyst surface. Therefore, it is highly interesting to apply these stable, colloidal PLAL-AuNPs with relatively "bare" surface in catalytic reactions in aqueous phase and compare their catalytic behavior with that of chemically synthesized ones, whose surfaces are always capped by a variety of stabilizing molecules (including bulky polymers). Besides, this —OH capped surface is supposed to easily interact with other materials, e.g., metal oxide with rich hydroxyl-group in aqueous solution, to form NP/metal-oxide hybrid structures which are of high relevance to practical applications. However, to date, research on PLAL-AuNPs has been mostly limited to the fabrication and surface chemistry investigations of NPs prepared under different conditions, such as laser parameters, solvents, pH values, and electrolytes [31–33,35]. The evaluation of their catalytic activities in various reactions is still lacking.

Here, we report a new method to prepare a nanostructured catalyst, which is composed of PLAL-AuNPs and CeO_2 NT support, and its application as highly active catalyst in the reduction of 4-nitrophenol (4-NP) into 4-aminophenol (4-AP), which is very useful for biomedicine and plastic industries [29,30,44]. The catalyst preparation method developed herein involves the fabrication of AuNPs (~5 nm in diameter) by PLAL and their uniform immobilization onto the CeO_2 NTs by simple mixing in solution, as illustrated in Scheme 1. Such a simple route does not require any additional surface modification processes to either AuNPs or CeO_2 NTs, while leading to extremely efficient anchorage of the NPs onto the tube surface. The PLAL-AuNPs/CeO_2-NTs demonstrate significantly superior catalytic activity in the 4-NP reduction reaction as compared with not only similar catalysts consisting of Chem-AuNPs or commercial CeO_2 powder, but also other supported Au catalysts reported recently by other groups. Besides, they also show excellent catalytic activity in the CO catalytic oxidation reaction in gas phase. Their remarkable catalytic activity is attributed to the relatively "bare" surface of the PLAL-AuNPs as well as to the strong

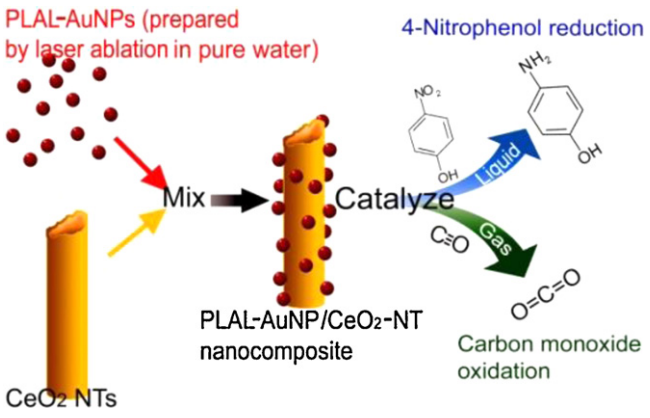

Scheme 1. Schematic diagram of the simple route for preparation of PLAL-AuNP/CeO_2-NT catalyst and its application in 4-NP reduction and CO oxidation.

Au-support interaction associated with the unique surface feature of both PLAL-AuNPs and CeO_2 NTs. Our novel PLAL-AuNPs/CeO_2-NTs are expected to be applicable as a highly efficient catalyst in many other catalytic reactions where AuNPs are involved. It should be possible to extend this simple strategy for the preparation of metal oxide supported nanocatalysts containing AuNPs to the preparation of other nano-heterostructures containing PLAL-metal NPs. This will open the door for PLAL-NPs to a wide variety of applications in catalysis.

2. Experimental

2.1. Materials

Gold plate target (99.99%), hydrogen tetrachloroaurate hydrate (auric acid, $HAuCl_4{\cdot}3H_2O$), sodium citrate, sodium borohydride ($NaBH_4$), cerium (III) nitrate hexahydrate ($Ce(NO_3)_3{\cdot}6H_2O$), urea (NH_2CONH_2), sodium hydroxyl (NaOH), nitric acid (HNO_3), 4-nitrophenol, cerium (IV) oxide powder (mean size ~500 nm) were purchased from Sigma–Aldrich and used without further purification. Pressure syringe filter composed of celluloid membrane filters (0.2 μm) and pressure filter-holder, and centrifuge filters (Amicon Ultra-4 Ultracel-50K) made by EMD Millipore Cooperation were obtained from Fisher Scientific. Water was purified by a Millipore Ultrapure water system and has a resistivity of 18.2 MΩ cm at 25 °C.

2.2. Preparation of PLAL-AuNPs

Laser ablation was carried out with a KrF excimer laser (GSI Lumonics PM-846, wavelength: 248 nm, repetition rate 20 Hz). The beam was focused by an objective lens, with a focal length of 7.5 cm, onto a gold plate with a diameter of 8 mm and 1.5 mm in thickness. The gold target was placed at the bottom of a 6 mL glass vessel filled with pure water (pH ≈ 6.5). The depth of the water layer above the target was ~10 mm. Laser fluence on the target was set at ~40.0 J/cm^2 during all ablation process.

2.3. Synthesis of CeO_2 NTs [54,55]

In a typical experiment, 1.736 g of $Ce(NO_3)_3{\cdot}6H_2O$ and 1.44 g of urea were added to 80 mL of water under vigorous magnetic stirring. The clear solution was charged into a 100 mL wide-mouthed jar which was closed and baked at 80 °C for 24 h. The solution was then air-cooled to room temperature. The obtained white powder was then centrifuged, washed with distilled water, and dried at 60 °C. It (0.087 g) was subsequently re-dispersed into 20 mL of distilled water. Upon addition of 2.4 g of NaOH, the mixture solution

was stirred for 30 min and then kept at room temperature. After 4 days of aging, the light yellow precipitation was washed with 1 M of HNO_3 solution, distilled water, and absolute ethanol sequentially, and then it was dried in a vacuum at 60 °C for 24 h for the following catalyst preparation.

2.4. Synthesis [56] and purification of Chem-AuNPs

One milliliter of 1 wt% $HAuCl_4{\cdot}3H_2O$ aqueous solution was added into 90 mL of deionized water, followed by injection of 2 mL of 38.8 mM sodium citrate solution. The reaction mixture was then stirred for 1 min. Subsequently, 1 mL of 0.075 wt% freshly prepared $NaBH_4$ solution (in 38.8 mM sodium citrate solution) was added and then the reaction mixture was stirred overnight at room temperature. After that, all as-synthesized Au colloidal solution was purified to remove any un-attached or un-reacted chemical species, and then 93 mL of 1.25 mM sodium citrate solution was loaded and sonicated to have AuNPs well re-dispersed for the following operation. Consequently, a delicate purification process was performed to the as-prepared Chem-AuNPs solution by using ultra-centrifuge filters. In a typical operation, 12 mL of as-prepared Au colloidal solution was centrifuged at ~4500 rpm with ultra-centrifuge filters into ~4 mL concentrated solution (8 mL of filtrate was discarded). And then ~8 mL of pure water was introduced to re-disperse the 4 mL highly concentrated AuNPs. After this pre-purification, additional washing operation was repeated gently twice in the same way. Final AuNPs were re-dispersed in pure water and used immediately for hybridization and characterization.

2.5. Fabrication of AuNP/CeO_2 catalysts

To 20 mg of CeO_2 NTs (or powder), 2 mL of freshly prepared PLAL-AuNPs solution (or purified Chem-AuNPs) was added and mixed by shaking. The mixture solution was incubated at room temperature for 30 min. After this, the pink precipitate was recovered by centrifugation, followed by washing with distilled water twice. Thus, the AuNP/CeO_2 catalyst was obtained.

2.6. Catalytic reduction of 4-NP

The aqueous solutions of 4-NP (0.12 mM) and $NaBH_4$ (5 mM) were freshly prepared. Typically, in a 50 mL flask, 10 mg of AuNP/CeO_2 catalyst (containing 0.031 mg of Au) was added to 15 mL of 4-NP aqueous solution. Subsequently, 15 mL of $NaBH_4$ solution was mixed with the 4-NP solution containing AuNP/CeO_2 nanocomposite under continuous stirring. The molar ratio of Au:4-NP:$NaBH_4$ in this catalytic reaction was about 1:11:462. All catalytic reactions were carried out at room temperature. In order to monitor the reaction, 1.5 mL of the reaction solution was taken out using a syringe every 60 s, and injected into a quartz cuvette immediately through a pressure syringe filter, which can separate catalyst from the reaction solution and terminate the reaction. The filtrate solution was then measured with the UV–vis absorption spectrometer.

2.7. Catalytic oxidation of CO

Catalytic activity was measured using a continuous flow fixed-bed micro-reactor at atmospheric pressure. In a typical experiment, the system was first purged with high purity N_2 gas and then a gas mixture of $CO/O_2/N_2$ (1:10:89) was introduced into the reactor containing 50 mg of AuNPs/CeO_2-NTs (1 wt% Au loading) at a flow rate of 33.6 mL/min (corresponding to a space velocity of 40,000 mL h^{-1} g^{-1} of catalyst), which were pre-annealed at 200 °C for 2 h. Gas samples were analyzed with an online infrared gas analyzer, which simultaneously detects CO and CO_2 with a resolution of 10 ppm. The results were further confirmed with a Gas Chromatograph.

2.8. Characterization

A UV–Visible (UV–vis) spectrometer (Varian 5000) was used to measure the absorption spectra of AuNPs and catalytic reaction solution at room temperature. Transmission electron microscopy (TEM) images were taken with a JEOS-2100F TEM (École Polytechnique de Montréal, Montréal, Canada) by drop casting sample dispersions on carbon-coated copper grids. X-ray photoelectron spectroscopy (XPS) spectra were performed using ESCA Escalab 220i XL with a polychromated Al Kα X-ray source (1486.6 eV) [34]. Elemental analysis with neutron activation analysis (NAA) technique was performed using SLOWPOKE nuclear reactor (École Polytechnique de Montréal, Montréal, Canada) to quantify Au component in the AuNPs/CeO_2 nanostructures, and to determine the amount of catalysts used in each reaction. Thermogravimetric analysis (TGA) was performed in air with a TA Instrument TGA Q500 thermogravimetric analyzer. CeO_2 NT surface area was measured with Quantachrome Autosorb System using nitrogen. The pH values of the solutions were measured with a Mettler-Toledo FG2 pH meter. Gas analyzer (Gasboard-3121, China Wuhan Cubic Co.) and Gas Chromatograph (Shimadzu, GC-14C) were employed to determine and confirm the gas composition in CO oxidation reaction, respectively.

3. Results and discussion

3.1. Preparation and structural characterization of PLAL-AuNP/CeO_2-NT nanocatalyst

A simple, functionalization-step-free solution process has been established to fabricate the AuNP/CeO_2 nanocatalyst. First, PLAL-AuNPs with diameter of ~5 nm were fabricated by laser ablation on a bulk Au target in pure water without any additional chemicals. Meanwhile, CeO_2 NTs were synthesized through a solid–liquid interface reaction between $Ce(OH)CO_3$ nanorods, which serve as template, and NaOH solution to first form a CeO_2 shell, and then followed by acid dissolution of residual $Ce(OH)CO_3$ precursor in the core according to our previous reports [54,55]. Second, the as-prepared PLAL-AuNP solution was simply mixed with the CeO_2 NTs and incubated for 30 min to assemble AuNPs onto the tube's surface. Fig. 1(a) shows the UV–vis absorption spectra of freshly prepared PLAL-AuNP solution before (solid line) and 30 min after the introduction of the CeO_2 NTs (dashed line), respectively. Before the addition of CeO_2 NTs, the UV–vis spectrum of PLAL-AuNP solution presents a strong Surface Plasmon Resonance (SPR) peak at ~513 nm. After mixing with the CeO_2 NTs, the PLAL-AuNPs demonstrate significantly strong affinity to the CeO_2 NTs, reflected from the dramatic decrease of their SPR peak at 513 nm. Nearly all PLAL-AuNPs are adsorbed onto the NT surface and together they precipitate from the solution. Correspondingly, this considerable difference in the optical absorption of the PLAL-AuNPs in the presence of the CeO_2 NTs is visible in its photographs shown in the insets of Fig. 1(a). The percentage of "free" (i.e., un-attached) AuNPs in the supernatant (deduced from the absorbance of the SPR peak at 513 nm) as a function of incubation time is summarized and illustrated in Fig. 1(c) (circles). It is found that most (~90%) of the AuNPs are adsorbed on the surface of the NTs within 10 min. Lengthening the incubation time to 30 min leads to the complete attachment. Consistently, it was found that the amount of Au element in the colloidal solution before mixing with CeO_2 NTs is the same as that in the fabricated nanocomposite (confirmed by NAA), which indicates

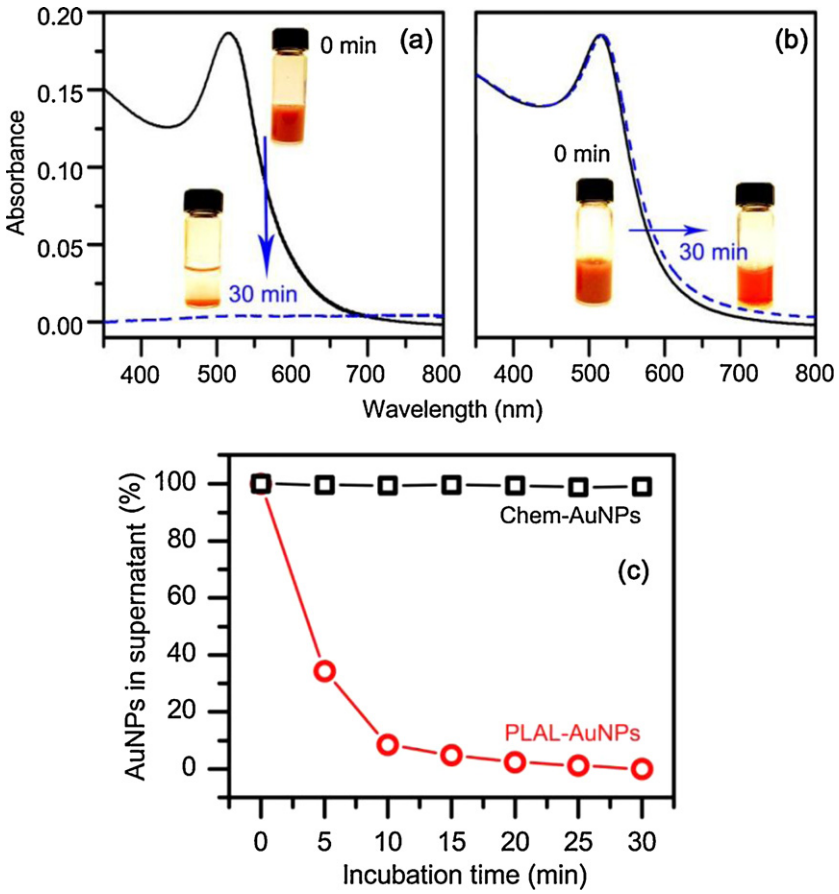

Fig. 1. UV–vis spectra of PLAL-AuNPs (a) and Chem-AuNPs (b) solution at 0 min (solid line) and 30 min (dash line) after the addition of CeO_2 NTs. (c) "Free" AuNPs remaining in the solution as a function of incubation time. Insets are corresponding photo-images.

that with this technique AuNPs entirely attach onto the support without any loss and thus the Au/CeO_2 ratio can be accurately controlled by simply varying the amount of feeding Au colloidal solution.

Of technical importance is that this preparative method for the AuNP/CeO_2 nanocomposite does not require any additional functionalization pretreatments to either AuNP or CeO_2 to promote their coupling. The effective immobilizing process is associated with the surface chemistry of the PLAL-AuNPs and CeO_2 NTs. Since the pH value of the incubation solution (pure water) is ~6.5 which is lower than the Isoelectric Point (IEP) of CeO_2 (7.0–7.6) [50], the surface of CeO_2 is partially positively charged [50]. On the other hand, the PLAL-AuNPs are negatively charged due to —OH adsorption [31–33]. Thus, the electrostatic interaction and hydrogen bonding between them lead to the formation of the AuNP/CeO_2 hybrid structure [28]. In terms of nanocomposite fabrication, the unique surface chemistry of PLAL-AuNP does appear advantageous.

Fig. 2(a)–(c) shows the TEM images of the PLAL-AuNPs/CeO_2-NTs. The tubular structure of CeO_2 is quite apparent (Fig. 2(a) and (b)) and at a higher magnification (Fig. 2(b)), the attachment of the PLAL-AuNPs on the tube surface can be clearly observed. The NPs are well distributed on the surface, and no unattached, individually dispersed AuNPs are observed, indicating that the PLAL-AuNPs have good affinity with the CeO_2 NTs. The AuNP/CeO_2-NT nanostructures were further characterized by high-resolution TEM (HR-TEM); as shown in Fig. 2(c), the lattice fringes of an attached AuNP with a diameter of ~5 nm and a CeO_2 NT surface are visible, with the spacing of 2.34 Å corresponding to that of the {1 1 1} planes of face-centered cubic Au [51] and the larger lattice spacing of 3.12 Å matching that of the {1 1 1} crystal planes of cubic fluorite-structured CeO_2 [51] These results regarding crystalline structures are consistent with those obtained from selected area electron diffraction (SAED) pattern shown in the inset of Fig. 2(a). The PLAL-AuNPs/CeO_2-NTs were also characterized by energy dispersive X-ray spectroscopy (EDS), which reveals the coexistence of both Au and Ce in the nanostructure as presented in Fig. 2(d).

3.2. *Catalytic activity of PLAL-AuNP/CeO_2-NT nanocatalyst for 4-NP reduction*

The catalytic property of the PLAL-AuNPs/CeO_2-NTs was then evaluated by employing the reduction of 4-NP into 4-AP, in which $NaBH_4$ was used as a reducing agent. During the catalytic reaction, active hydrogen species are firstly transferred to the surface of AuNPs by borohydride, and then the reduction of 4-NP takes place by the reaction of adsorbed 4-NP molecules and surface-hydrogen. In this study, since $NaBH_4$ was added to the reaction in large excess as compared to 4-NP, the reaction kinetics basically follows a first-order rate law [41–44]. The kinetic process of the reaction was monitored by measuring the absorbance of a peak at 400 nm ($Abs_{400\,nm}$), directly associated with the concentration of 4-nitrophenolate ions, as a function of reaction time. Fig. 3(a) shows that after the addition of the catalyst, the $Abs_{400\,nm}$ value drops gradually as the reaction proceeds, reflecting the steady decrease of the concentration of the 4-nitrophenolate ions in solution. Based on the absorbance data, Fig. 3(b) plots the C/C_0 (square) and $-\ln(C/C_0)$ (circle) vs. reaction time, where C_0 and C are the initial concentration of the 4-nitrophenolate ions and the concentration at time t, respectively. The reaction is almost complete within 1200 s in the presence of the PLAL-AuNP/CeO_2-NT catalyst. The linear

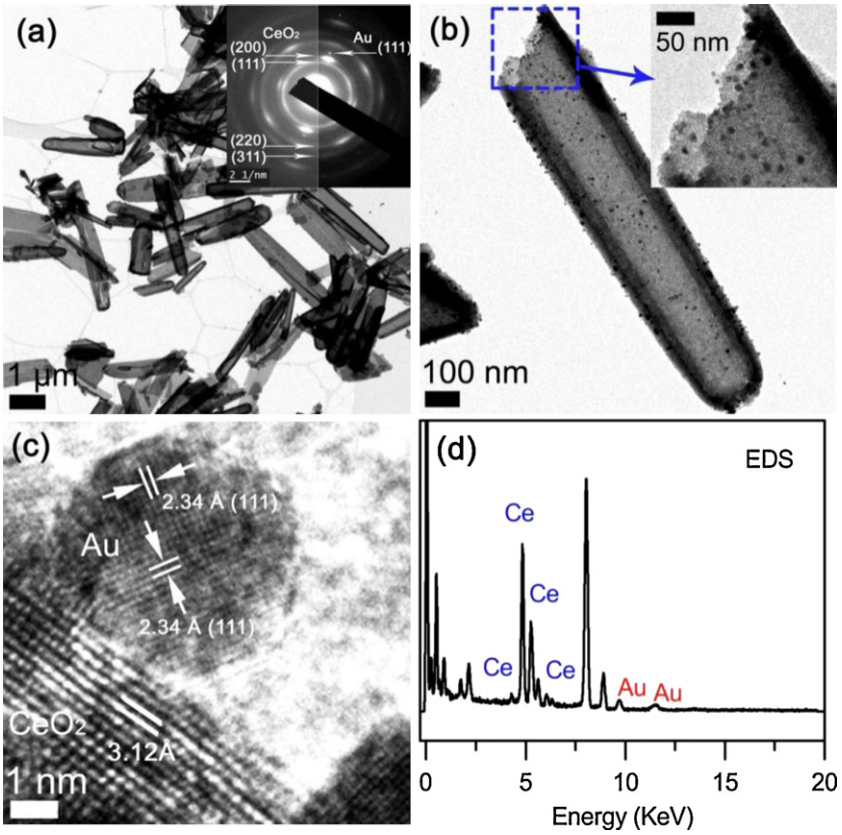

Fig. 2. TEM (HR-TEM) images (a-c) and EDS spectrum (d) of PLALAuNPs/CeO_2-NTs. Insets are the SAED pattern and the magnified TEM image.

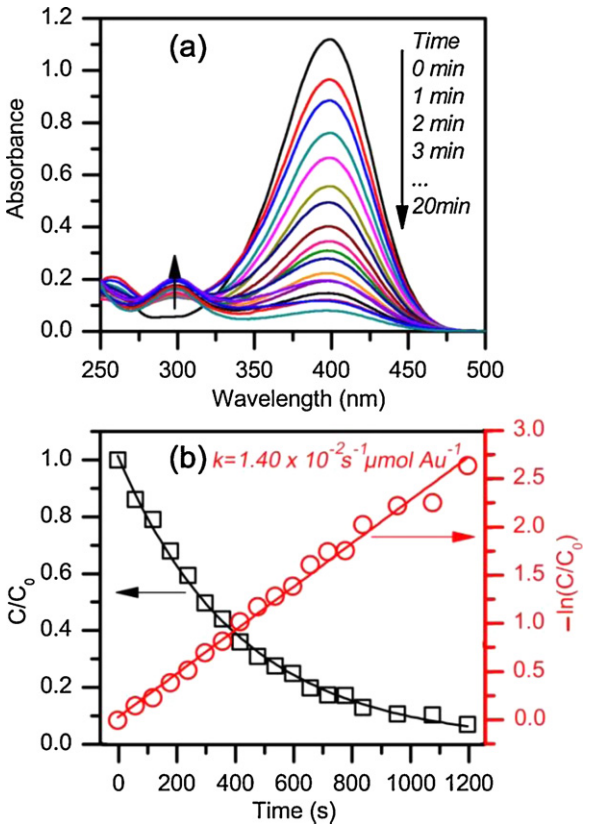

Fig. 3. (a) UV–vis absorption spectra during the catalytic reduction of 4-NP over PLAL-AuNPs/CeO_2-NTs; (b) C/C_0 and $-\ln(C/C_0)$ as a function of reaction time for the reduction of 4-NP over PLAL-AuNPs/CeO_2-NTs.

correlation between $-\ln(C/C_0)$ and reaction time demonstrates that the reaction is of the first-order in 4-NP reduction. Thus, the kinetic equation of this catalytic reaction could be shown as follows

$$\frac{dC}{dt} = -k_{app}C$$

where k_{app} is the apparent reaction rate constant, which can be obtained from the slope of the linear correlation [43,44,49]. Accordingly, the k_{app} for the PLAL-AuNPs/CeO_2-NTs catalyzed reaction was calculated to be $2.25 \times 10^{-3}\ s^{-1}$. To exclude the effect of Au loading on reaction efficiency, and also for fair comparison with the results reported by other groups on AuNP based catalysts, an intrinsic reaction rate constant, k, was introduced by further normalizing k_{app} with Au content [41,49]:

$$k = \frac{k_{app}}{M}$$

where M is the dosage of Au (μmol) in the catalyst. It was found that k ($1.40 \times 10^{-2}\ s^{-1}$ μmol Au^{-1}) of the PLAL-AuNPs/CeO_2-NTs is impressively higher than those reported recently by others on Au-containing nanocatalysts (see Table S1 for summary) [44–49].

3.3. Mechanism for enhanced catalytic activity

In order to understand why the PLAL-AuNPs/CeO_2-NTs show superior catalytic activty, we prepared similar catalysts containing citrate ligand-capped AuNPs synthesized via a common chemical reduction method (Chem-AuNPs) and/or commercial CeO_2 nanopowder support, and then compared their catalytic activity with that of the PLAL-AuNPs/CeO_2-NTs.

3.3.1. Surface chemistry of NPs: PLAL vs. Chem-AuNPs

To guarantee a fair comparison, it is necessary to exclude particle size effect. Therefore, citrate ligand-capped Chem-AuNPs with the same particle size were prepared by reducing $HAuCl_4$ with $NaBH_4$ in citrate solution (see Section 2) [56]. TEM observation (Fig. S1(a) and (b) in supplementary data) shows that as-prepared PLAL-AuNPs and purified Chem-AuNPs have a very similar size (~5 nm in diameter) and size distribution. This was further confirmed by their identical SPR peak position and similar full width at half-maximum (Fig. S1(c)).

The Chem-AuNPs and the CeO_2 NTs are then mixed under the same experimental conditions as those applied for preparing the PLAL-AuNPs/CeO_2-NTs. Fig. 1(b) shows the UV–vis spectra and photographs of the as-prepared Chem-AuNP solution before (solid line) and 30 min after (dashed line) the addition of the CeO_2 NTs. It is clear that unlike the PLAL-AuNPs, the Chem-AuNPs do not attach to the CeO_2 NTs (black square, Fig. 1(c)).

Abundant "free" citrate molecules in solution have been found necessary to stabilize Chem-AuNPs. Therefore, in general, they are kept in solution for the manipulation of the Chem-AuNPs (such as surface functionalization); otherwise rapid aggregation can easily take place [52]. Based on this consideration, the Chem-AuNPs, which were only purified once to remove un-reacted chemical species and then dispersed in 1.25 mM of sodium citrate solution, were used for coupling with the CeO_2 NTs. Unfortunately, this "standard" stable Au colloidal solution seems inappropriate for the current coupling reaction. Quite likely, free citrate ions in solution are easily adsorbed onto the positively charged CeO_2 NT surface, leading to the formation of a negatively charged surface that hinders the adsorption of negatively charged Chem-AuNPs [27].

To promote the coupling yet avoiding rapid NP agglomeration, a delicate purification/washing protocol was developed for as-prepared Chem-AuNPs (see Section 2). Our study shows that the Chem-AuNPs with ~0.9 wt% of the citrate ligand content (measured by TGA) can rapidly adsorb on the surface of CeO_2 without evident aggregation. Although successful, the manipulation of the Chem-AuNPs for the catalyst preparation is obviously less convenient and more time-consuming, with respect to the PLAL-AuNPs.

The same amount of the Chem-AuNPs as that of the PLAL-AuNPs was coupled with the NTs (examined by NAA) for comparison of catalytic activity. Inset of Fig. 4(b) presents a typical TEM image of the Chem-AuNPs/CeO_2-NTs, whose structure is similar to that of the PLAL-AuNPs/CeO_2-NTs. Fig. 4(a) shows the evolution of the UV–vis spectra of the 4-NP reaction solution when the Chem-AuNPs/CeO_2-NTs are used as a catalyst. It can be seen that the absorbance of 4-nitrophenolate ions only decreases by half after 1800 s in the presence of the Chem-AuNPs/CeO_2-NTs, while it drops to ~0 after the same reaction time in the case of the PLAL-AuNPs/CeO_2-NTs. Fig. 4(b) displays the variation of C/C_0 and $-\ln(C/C_0)$ with the reaction time as derived from Fig. 4(a). Both values vary less severely than those shown in Fig. 3(b), indicating a lower reaction efficiency. The k value of the Chem-AuNPs/CeO_2-NTs is 2.86×10^{-3} s^{-1} μmol Au^{-1}, about 5 times smaller than that of the PLAL-AuNPs/CeO_2-NTs. It is noted that, the PLAL-AuNP/CeO_2-NT catalyst still keeps rather good catalytic activity after four rounds of successive reactions, and its k value for each round is much higher than that of the Chem-AuNP/CeO_2-NT catalyst as well (Fig. S2). Clearly, chemically synthesized, citrate-capped AuNPs exhibit considerably inferior catalytic activity than the PLAL-AuNPs that have relatively "bare" surface. As the PLAL-AuNPs and Chem-AuNPs have similar size distribution and their hybrids with the NTs have the similar structure and Au/support ratio, the quite different catalytic activity for the same reaction must therefore be related to inherent difference between these two types of AuNPs, rather than the morphology of the catalysts.

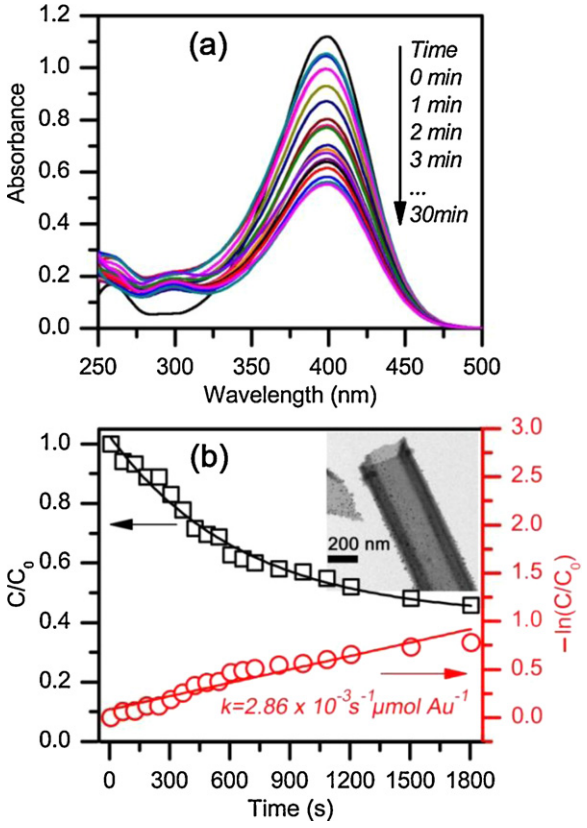

Fig. 4. (a) UV–vis absorption spectra during the catalytic reduction of 4-NP over Chem-AuNPs/CeO_2-NTs; (b) C/C_0 and $-\ln(C/C_0)$ as a function of reaction time for the reduction of 4-NP over Chem-AuNPs/CeO_2-NTs. Inset shows the TEM image of the Chem-AuNPs/CeO_2-NTs.

As described above, after careful purification, most free ligands are removed from the solution. Nonetheless, the Chem-AuNPs are still covered by certain amounts of citrate ligands. They could directly passivate the reactive sites or prohibit the access of reactant molecules to the reactive sites by providing spatial hindrance. As a consequence, more surface sites of the Chem-AuNPs that should be catalytically active are blocked, resulting to the lower catalytic activity as compared with the relatively "bare" PLAL-AuNPs. In contrast, the small —OH groups on the latter NP surface leave more surface sites available for reactants. It is clear that the use of the PLAL-AuNPs is not only beneficial for the easy, time-saving, effective conjugation with the NTs, but also contributes to the increase of catalytic activity. The blocking effect of the PLAL-AuNPs in catalysis is much less, if any, than that of citrate, which are commonly used in AuNP preparation and are indeed already small stabilizing agents. The above observations indicate that the surface chemistry of AuNPs is very important for coupling and catalytic performance.

3.3.2. Au-support interaction: CeO_2-NT vs. commercial ceria powder

NTs have been considered as interesting support materials for catalytic NPs because their geometry provides a relatively high surface area to volume ratio for better dispersion of NPs. In our case, besides the advantage of the high surface area of CeO_2 NTs, it is anticipated that their interaction with Au may also partially contribute to the excellent catalytic activity of the PLAL-AuNPs/CeO_2-NTs [7,13,54]. To examine that, commercial ceria nanopowder was introduced as support to disperse and stabilize PLAL- and Chem-AuNPs, and the same preparation procedures as those applied for the CeO_2 NTs were adopted to fabricate the nanocomposites. The insets in Fig. 5(a) and (b) displays the TEM

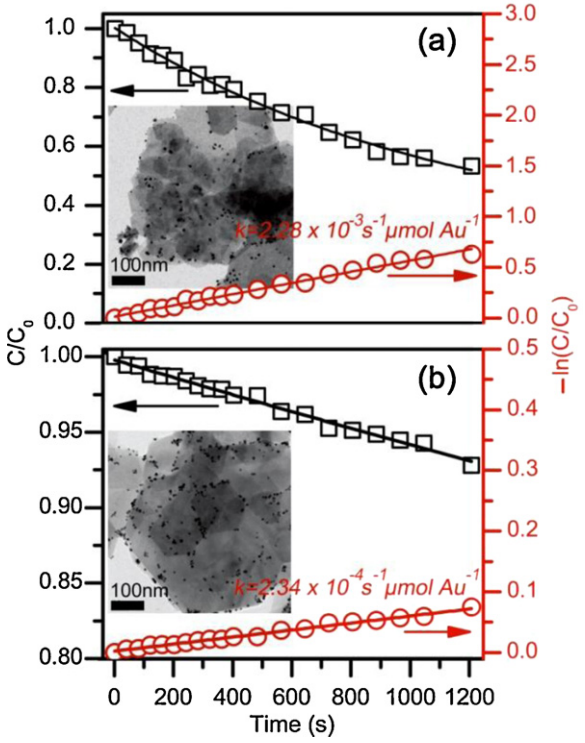

Fig. 5. C/C_0 and $-\ln(C/C_0)$ as a function of reaction time for the reduction of 4-NP over PLAL-AuNPs/CeO_2-powder (a) and Chem-AuNPs/CeO_2-powder (b), respectively. Insets show the corresponding TEM images of nanocatalyst (a) and (b).

images of the PLAL-AuNPs/CeO_2-powder and Chem-AuNPs/CeO_2-powder, respectively. No obvious aggregation of AuNPs was observed and both types of AuNPs disperse well on the surface of CeO_2 particles. The variation of their C/C_0 and $-\ln(C/C_0)$ with reaction time during the reduction of 4-NP is shown in Fig. 5(a) and (b), respectively. The k value of the PLAL-AuNPs/CeO_2-powder is nearly 10 times higher than that obtained for the Chem-AuNPs/CeO_2-powder, again indicating that the PLAL-AuNPs are more active than the Chem-AuNPs. However, both k values are far below those achieved when the CeO_2 NTs are used as support. Specifically, the k value of $1.40 \times 10^{-2}\ s^{-1}\ \mu mol\ Au^{-1}$ for the NT supported PLAL-AuNPs is about 6 times higher than that of the CeO_2 powder supported PLAL-AuNPs ($2.28 \times 10^{-3}\ s^{-1}\ \mu mol\ Au^{-1}$). These results strongly suggest that the CeO_2 NTs, as supports, have positive impact on the catalytic activity; they are at least partially responsible for the significantly higher catalytic activity of the PLAL-AuNPs/CeO_2-NTs in the 4-NP reduction reaction as compared with other Au-containing catalysts [44–49], including those investigated herein.

The surface area of the CeO_2 NTs is ~74 m^2/g (Fig. S3), which is much higher than that of commercial powders (~1.58 m^2/g). The higher reaction rate with the former sample may thus be simply attributed to the better dispersion of NPs and thus more effective contact with the reactants. However as AuNPs are uniformly distributed without aggregation (insets of Figs. 4 and 5) and are loaded at the same level in both cases, the surface area difference of CeO_2 supports should not be the dominant factor for the significant difference in catalytic activity observed herein. Instead, the Au-support interaction may play a critical role herein [2–4,7–25].

To test this hypothesis, XPS was used as an effective surface analysis tool, to analyze the surface chemistry of both CeO_2 supports and AuNPs. Fig. 6(a) shows the Ce $3d_{5/2}$ XPS spectra of CeO_2 NTs and commercial CeO_2 powder. The proportion of Ce^{3+} indicated by the peak at ~885.8 eV [54] in the NTs is considerably higher than that

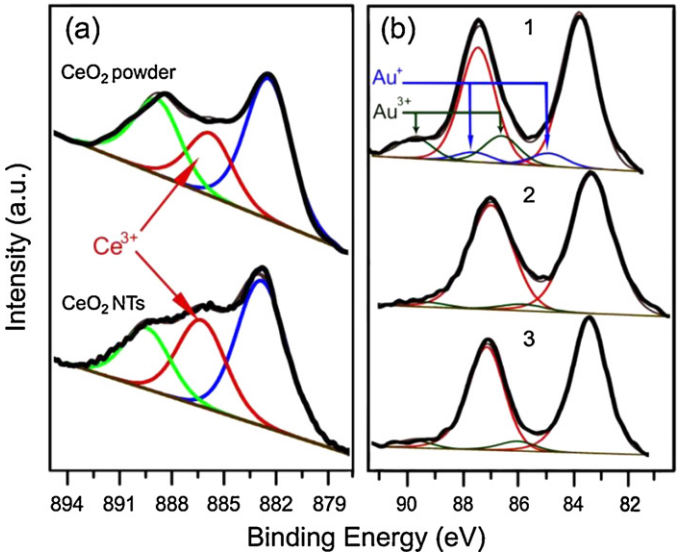

Fig. 6. XPS spectra of Ce $3d_{5/2}$ (a) for CeO_2 supports and Au 4f (b) of PLAL-AuNPs/CeO_2-NTs (1), PLAL-AuNPs/CeO_2-powder (2) and Chem-AuNPs/CeO_2-NTs (3). (For interpretation of the references to color in the text, the reader is referred to the web version of this article.)

in the commercial powder, suggesting that there are more defects (i.e., oxygen vacancy) enriched on the NT surface [7–10,13,26,40]. It is well-known that the surface defects in CeO_2 can strongly interact with Au atoms to modify their electronic structure and stabilize the oxidation states of Au [7–10,13]. These oxidized species have been found to play a positive role in the reduction of 4-NP [43]. From this point of view, it is interesting to examine the chemical status of Au in our nanocomposites. The XPS spectra of Au 4f were thus taken on the PLAL-AuNPs/CeO_2-NTs, PLAL-AuNPs/CeO_2-powder and Chem-AuNPs/CeO_2-NTs. As shown in Fig. 6(b), all deconvoluted Au 4f spectra exhibit two main peaks (red doublet) corresponding to metallic Au^0 [53]. For the PLAL-AuNPs/CeO_2-NTs (curve 1), in addition to metallic Au^0, broadened shoulders on the high binding energy side are composed of four distinct additional peaks (blue and green doublets), which can be assigned to the oxidation state of Au (Au^+ and Au^{3+}) [7]. As compared with the Au 4f spectrum of the PLAL-AuNPs/CeO_2-NTs, the intensity of oxidized Au species of the PLAL-AuNPs/CeO_2-powder (curve 2) and Chem-AuNPs/CeO_2-NTs (curve 3) is much lower. Because the Au oxidation states were not observed for unsupported PLAL- and Chem-AuNPs in their XPS spectra (Fig. S4), the relatively high content of oxidized Au species in the PLAL-AuNPs/CeO_2-NTs must originate from the strong Au/CeO_2-NT interaction [7–10], which is induced by the defect-enriched CeO_2 NTs [18] and enabled by the highly intimate contact of "bare" AuNPs and CeO_2 [18]. In contrast, this interaction is weaker in the hybrids containing either the Chem-AuNPs or CeO_2 powder due to the steric hindrance effect from the citrate ligand on the Chem-AuNPs and less oxygen vacancies in the CeO_2 powder, explaining the much lower content of the oxidized Au species in these two samples. The PLAL-AuNPs and CeO_2 NTs together contribute to the strong Au–CeO_2 interaction. The oxidized Au species arising from this interaction may act as electron relay system, which accelerates the electron transfer from BH_4^- to 4-NP in the hydrogenation process [43], leading to the superior catalytic performance of the PLAL-AuNPs/CeO_2-NTs.

3.4. PLAL-AuNPs/CeO_2-NTs toward CO oxidation

To further illustrate the unique, advantageous feature of the PLAL-AuNPs/CeO_2-NTs in catalytic reactions, we also studied their

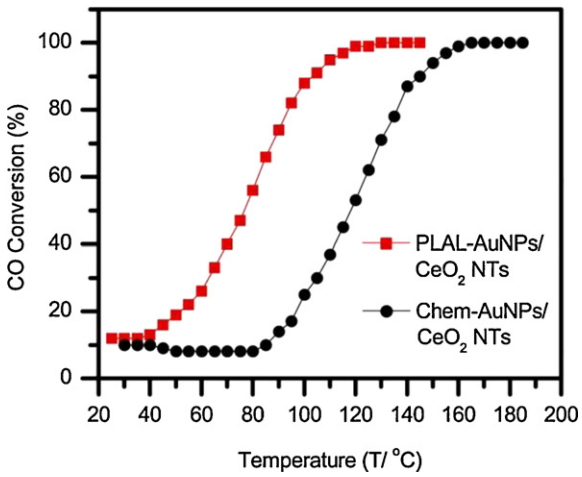

Fig. 7. Temperature dependence of CO conversion in CO oxidation reaction over PLAL-AuNPs/CeO_2-NTs and Chem-AuNPs/CeO_2-NTs.

catalytic activity toward CO oxidation, which has attracted extensive research due to its fundamental importance in air purification. Fig. 7 shows the activity curve of the annealed PLAL-AuNPs/CeO_2-NTs along with that of Chem-AuNPs/CeO_2-NTs for comparison. The PLAL-AuNPs/CeO_2-NTs exhibit higher catalytic efficiency at the same temperature. The reaction rate with the presence of these two catalysts was further calculated at low conversions. For example, at ~45 °C the CO conversion reaches ~15% with the use of the PLAL-AuNPs/CeO_2-NTs in contrast to ~8% with the Chem-AuNPs/CeO_2-NTs. Accordingly, the reaction rate for the CO oxidation at this temperature proceeding over these two catalysts was calculated to be ~0.42 and ~0.22 mmol CO_2 min^{-1} mg^{-1}, respectively. The reaction rate upon PLAL-AuNPs/CeO_2-NTs is comparable with those calculated from other reports using solely chemically prepared AuNP/CeO_2 catalysts [22–25]. Since the CeO_2 NT support, and the size and morphology of both types of AuNPs are the same, the higher catalytic activity of the former sample can be attributed to the bare surface of the PLAL-AuNPs and the strong Au-support interaction [7–10]. The benefit of the bare surface of catalysts in catalysis is expected in most catalytic reactions. As for the contribution of the Au–CeO_2 interaction, it has been well-studied and largely reported for small molecule oxidation reactions [8–11,13–15,18,20–26]. For example, by studying Au–CeO_2 and Au–SiO_2 multilayer nanostructures in CO oxidation, Zhou et al. experimentally identified that the active sites for this catalytic reaction are located at the interface of Au and CeO_2 [8]. They further found that the extremely low activity of a pure Au thin film in CO oxidation can be enhanced remarkably by decorating it with Ce^{3+}-rich CeO_2 NPs since the strong interaction occurring at the interface of CeO_2 NPs and Au surface induces a significant increase of the active sites on Au surface [9]. In our study, as shown in the XPS part, the CeO_2 NTs containing higher concentration of Ce^{3+} defect couple directly with the relatively "bare and clean" PLAL-AuNPs without suffering from any steric hindrance, resulting in a stronger interaction at the CeO_2–Au interface than that in the samples containing either the Chem-AuNPs or CeO_2 powder. This strong interaction leads to an increase of catalytically active sites, as reflected in the XPS as a higher concentration of Au in oxidation states. The positive role of oxidized Au species at the interface introduced by the strong interaction in CO oxidation has been widely accepted because they promote CO_2 desorption in the CO oxidation process [7,10]. An interesting question arises: will the Ce^{3+} defect concentration change during and after CO oxidation? Lee et al. found that Ce^{3+} (oxygen vacancy) content of Au–CeO_2 nanorods catalyst does not change obviously in the presence of O_2 during reaction, whereas it decreases without O_2 by monitoring the reaction with Raman scattering [26]. In another report, the Ce^{3+} concentration of very small CeO_2 NPs (~5 nm) deposited on Au film was found to decrease after CO oxidation [9]. As Ce^{3+} concentration is believed to be directly related to catalytic activity as well as long-term stability of the catalysts reported herein, the investigation on its variation with catalytic reactions is ongoing.

4. Conclusion

In summary, a highly catalytically active AuNP/CeO_2-NT nanocomposite was synthesized by simply mixing laser ablated Au colloids with CeO_2 NTs. Due to the OH^- group on the AuNP surface resulting from laser ablation process, the PLAL-AuNPs show good affinity with CeO_2. The PLAL-AuNPs/CeO_2-NTs exhibit high catalytic activity in the reduction of 4-NP in liquid phase and CO oxidation in gas phase. Based on the comparative studies on similar catalysts of the Chem-AuNPs/CeO_2-NTs, PLAL-AuNPs/CeO_2-powder, and Chem-AuNPs/CeO_2-powder, it is found that besides the relatively "bare" surface of the PLAL-AuNPs, the presence of relatively high content of the oxidized Au species induced by the strong interaction of the bare PLAL-AuNPs and the defects on the surface of the CeO_2 NTs additionally contributes to the superior activity of the PLAL-AuNPs/CeO_2-NTs. This catalyst could be applied to other catalytic reactions, such as degradation of organic molecules in waste water and exhaust gas, in which AuNPs are involved. This work represents the first demonstration of the use of PLAL-metal NPs in catalysis and the simple approach of preparing the nanostructured catalysts can potentially be extended to other hetero-nanostructured materials, made of PLAL-metal NPs (such as Pt and PtAu alloys) and metal oxide (such as TiO_2 and Al_2O_3). Such hetero-structured materials can find a wide range of applications including, but not limited to, catalysis.

Acknowledgements

The authors would like to acknowledge funding from the Natural Sciences and Engineering Research Council of Canada and Fonds de la recherche sur la nature et les technologies.

Appendix A. Supplementary data

Supplementary data associated with this article can be found, in the online version, at http://dx.doi.org/10.1016/j.apcatb.2012.11.030.

References

[1] M. Haruta, T. Kobayashi, H. Sano, N. Yamada, Chemistry Letters 16 (1987) 405.
[2] A. Corma, H. Garcia, Chemical Society Reviews 37 (2008) 2096.
[3] M.J. Climent, A. Corma, J.C. Hernández, A.B. Hungría, S. Iborra, S. Martínez-Silvestre, Journal of Catalysis 292 (2012) 118.
[4] M. Boronat, A. Corma, Langmuir 26 (2010) 16607.
[5] J.A. Lopez-Sanchez, N. Dimitritos, C. Hammond, G.L. Brett, L. Kesavan, S. White, P. Miedziak, R. Tiruvalam, R.L. Jenkins, A.F. Carley, D. Knight, C.J. Kiely, J. Hutchings, Nature Chemistry 3 (2011) 551.
[6] Q. Fu, H. Saltsburg, M. Flytzani-Stephanopoulos, Science 301 (2003) 935.
[7] R. Si, M. Flytzani-Stephanopoulos, Angewandte Chemie International Edition 47 (2008) 2884.
[8] Z. Zhou, S. Kooi, M. Flytzani-Stephanopoulos, H. Saltsburg, Advanced Functional Materials 18 (2008) 2801.
[9] Z. Zhou, M. Flytzani-Stephanopoulos, H. Saltsburg, Journal of Catalysis 280 (2011) 255.
[10] M.F. Camellone, S. Fabris, Journal of the American Chemical Society 131 (2009) 10473.
[11] N. Zheng, G.D. Stucky, Journal of the American Chemical Society 128 (2006) 14278.
[12] Y. Zhu, H. Qian, B.A. Drake, R. Jin, Angewandte Chemie International Edition 49 (2010) 1295.
[13] A. Abad, P. Concepcion, A. Corma, H. Garcia, Angewandte Chemie International Edition 44 (2005) 4066.

[14] C.G. Long, J.D. Gilbertson, G. Vijayaraghavan, K.J. Stevenson, C.J. Pursell, B.D. Chandler, Journal of the American Chemical Society 130 (2008) 10103.
[15] M. Comotti, W.-C. Li, B. Spliethoff, F. Schuth, Journal of the American Chemical Society 128 (2006) 917.
[16] X. Zhang, H. Shi, B.-Q. Xu, Angewandte Chemie International Edition 44 (2005) 7132.
[17] Z.-P. Liu, C.-M. Wang, K.-N. Fan, Angewandte Chemie International Edition 45 (2006) 6865.
[18] A. Horvath, A. Beck, G. Stefler, T. Benko, G. Safran, Z. Varga, J. Gubicza, L. Guczi, Journal of Physical Chemistry C 115 (2011) 20388.
[19] S. Ivanova, V. Pitchon, C. Petit, H. Herschbach, A. Van Dorsselaer, E. Leize, Applied Catalysis A: General 298 (2006) 203.
[20] Q. Xu, K.C.C. Kharas, A.K. Datye, Catalysis Letters 85 (2003) 229.
[21] S.C. Parker, C.T. Campbell, Topics in Catalysis 44 (2007) 3.
[22] M. Han, X. Wang, Y. Shen, C. Tang, G. Li, R.L. Smith, Journal of Physical Chemistry C 114 (2010) 793.
[23] G. Glaspell, L. Fuoco, M.S. El-Shall, Journal of Physical Chemistry B 109 (2005) 17350.
[24] A.M. Venezia, G. Pantaleo, A. Longo, G.D. Cario, M.P. Casaletto, F.L. Liotta, G. Deganello, Journal of Physical Chemistry B 109 (2005) 2821.
[25] P.X. Huang, F. Wu, B.L. Zhu, X.P. Gao, H.Y. Zhu, T.Y. Yan, W.P. Huang, S.H. Wu, D.Y. Song, Journal of Physical Chemistry B 109 (2005) 19169.
[26] Y. Lee, G. He, A.J. Akey, R. Si, M. Flytzani-Stephanopoulos, I.P. Herman, Journal of the American Chemical Society 133 (2011) 12952.
[27] A. Horvath, A. Beck, A. Sarkany, G. Stefler, Z. Varga, O. Geszti, L. Toth, L. Guczi, Journal of Physical Chemistry B 110 (2006) 15417.
[28] F. Xiao, F. Wang, X. Fu, Y. Zheng, Journal of Materials Chemistry 22 (2012) 2868.
[29] N. Sahiner, H. Ozay, O. Ozay, N. Aktas, Applied Catalysis B: Environmental 101 (2010) 137.
[30] S. Gazi, R. Ananthakrishnan, Applied Catalysis B: Environmental 105 (2011) 317.
[31] J.-P. Sylvestre, S. Poulin, A.V. Kabashin, E. Sacher, M. Meunier, J.H.T. Luong, Journal of Physical Chemistry B 108 (2004) 16864.
[32] F. Mafuné, J.-Y. Kohno, Y. Takeda, T. Kondow, Journal of Physical Chemistry B 107 (2003) 4218.
[33] G. Cristoforetti, E. Pitzalis, R. Spiniello, R. Ishak, M. Muniz-Miranda, Journal of Physical Chemistry C 115 (2011) 5073.
[34] J. Zhang, D. Riabinina, M. Chaker, D. Ma, Langmuir 28 (2012) 2858.
[35] J. Zhang, D.N. Oko, S. Garbarino, R. Imbeault, M. Chaker, A.C. Tavares, D. Guay, D. Ma, Journal of Physical Chemistry C 116 (2012) 13413.
[36] V.S. Burakov, A.V. Butsen, N.V. Tarasenko, Journal of Applied Spectroscopy 77 (2010) 386.
[37] A.K. Sinha, K. Suzuki, M. Takahara, H. Azuma, T. Nonaka, N. Suzuki, N. Takahashi, Journal of Physical Chemistry C 112 (2008) 16028.
[38] L. Guczi, A. Beck, K. Frey, Gold Bulletin 42 (2009) 5.
[39] L. Guczi, D. Horvath, Journal of Physical Chemistry B 104 (2000) 3183.
[40] I. Celardo, M.D. Nicola, C. Mandoli, J.Z. Pedersen, E. Traversa, L. Ghibelli, ACS Nano 5 (2011) 4537.
[41] T. Yu, J. Zeng, B. Lim, Y. Xia, Advanced Materials 22 (2010) 5188.
[42] K. Kuroda, T. Ishida, M. Haruta, Journal of Molecular Catalysis A: Chemical 298 (2009) 7.
[43] J. Huang, S. Vongehr, S. Tang, H. Lu, X. Meng, Journal of Physical Chemistry C 114 (2010) 15005.
[44] Z. Zhang, C. Shao, P. Zou, P. Zhang, M. Zhang, J. Mu, Z. Guo, X. Li, C. Wang, Y. Liu, Chemical Communications 47 (2011) 3906.
[45] Y. Xia, Z. Shi, Y. Liu, Polymer 51 (2010) 1328.
[46] Y.-C. Chang, D.-H. Chen, Journal of Hazardous Materials 165 (2009) 664.
[47] M.H. Rashid, T.K. Mandal, Advanced Functional Materials 18 (2008) 2261.
[48] M. Zhang, L. Liu, C. Wu, G. Fu, H. Zhao, B. He, Polymer 48 (2007) 1989.
[49] S. Panigrahi, S. Basu, S. Praharaj, S. Pande, S. Jana, A. Pal, S.K. Ghosh, T. Pal, Journal of Physical Chemistry C 111 (2007) 4596.
[50] P.L. Dubin, P. Tong, Colloid–Polymer Interactions: Particulate, Amphiphilic, and Biological Surfaces, American Chemical Society, Oxford University Press, NY, USA, 1993.
[51] JCPDS card file no. 00-004-0784 (Au) and 34-0394 (CeO_2).
[52] I. Ojea-Jimenez, V. Puntes, Journal of the American Chemical Society 131 (2009) 13320.
[53] V.B. Crist, PDF Handbooks of Monochromatic XPS Spectra, vol. 1: The Elements and Native Oxides, XPS, International, LLC, CA, USA, 1999.
[54] G. Chen, C. Xu, X. Song, W. Zhao, Y. Ding, S. Sun, Inorganic Chemistry 47 (2008) 723.
[55] G. Chen, F. Rosei, D. Ma, Advanced Functional Materials 18 (2012) 3914.
[56] W. Haiss, N.T.K. Thanh, J. Aveard, D.G. Fernig, Analytical Chemistry 79 (2007) 4215.